Carboxylate modification of sugarcane bagasse for effectively Cd(II) removal from aqueous solutions: a low-cost renewable and environment-friendly agricultural waste-based adsorbent

Jinzhen Ma[a], Ping Li[a,b,*], Su-nv Wang[a], Xiangyu Zheng[a], Jinhua Wu[a,b]

[a]*School of Environment and Energy, South China University of Technology, Guangzhou 510006, China,*
Tel./Fax: +86-20-39380568; emails: pli@scut.edu.cn (P. Li), Jinzhen_ma@163.com (J. Ma), 1939457822@qq.com (S.-n. Wang),
cyzxy@scut.edu.cn (X. Zheng), jinhuawu@scut.edu.cn (J. Wu)
[b]*The Key Lab of Pollution Control and Ecosystem Restoration in Industry Clusters, Ministry of Education,*
South China University of Technology, Guangzhou 510006, China

ABSTRACT

The toxic Cd(II) in aqueous solution is a poisonous ion and attracts much attention recently. Based on the conception of "treating waste with waste," carboxylate-functionalized sugarcane bagasse (CF-SCB) was successfully fabricated via a facile carboxymethylation process to absorb cadmium in wastewater as a low-cost and environment-friendly material. The chemical structure of CF-SCB were confirmed by scanning electron microscopy, energy dispersive X-ray, and Fourier-transform infrared, respectively. The influences of solution pH, adsorbent dosage, ionic strength, contact time, and the initial concentration of Cd(II) on the adsorption capacities were investigated in detail. The Cd(II) adsorption capacity of CF-SCB increased more than 10 times of pH 6 when the raw SCB was used as the control. The experimental adsorption data were best described by pseudo-second-order kinetic model and Langmuir isotherm with a maximum adsorption capacity of 134.23 ± 5.68 mg/g at pH 6 and 120.19 ± 4.28 mg/g at pH 4. Five-cycle reusability tests proved CF-SCB exhibited good reusability with a slight adsorption capacity loss (<11.6%). All the results revealed that the primary mechanism of Cd(II) adsorption was the ion exchange. This study paved a facile method to fabricate a cost-effective adsorbent CF-SCB, which presented excellent adsorption capability and reusability, which could be an enormous potential candidate for remediating wastewater polluted by cadmium ion.

Keyword: Cd(II); Adsorption; Carboxymethylation; Regeneration; Sugarcane bagasse

1. Introduction

The water environment has deteriorated significantly in the past decades [1]. In particular, heavy metals have become one of the major water pollution problems due to their toxicity, persistence, non-biodegradability, and bioaccumulation [2,3]. Among the heavy metal ions emitted, Cd(II) is considered to be a typical harmful pollutant. When enriched in the human body along the food chain, it will cause irreparable damage to various organs including tissues, the nervous, and the reproductive system [4,5]. Therefore, finding a suitable method to remove Cd(II) from contaminated wastewater is necessary to protect human health and water resources [6,7].

Various techniques such as ion exchange, phase extraction, chemical precipitation, membrane separation, biological treatment, and electrochemical methods have been widely used for the treatment of heavy metal pollution [8]. However, the above methods generally have inherent limitations such as low efficiency, long cycle, high cost,

* Corresponding author.

complicated operation, and secondary pollution, which limits their practical application [9,10]. Compared with other methods, the adsorption method has the advantages of high efficiency, low cost, and simple operation which makes it becomes one of the most successful methods to remove cadmium ions from wastewater [11,12]. Multitudinous adsorbents such as activated carbon, nanomaterials, industrial, and agricultural wastes have been used to remove Cd(II) during the past several decades [13–17]. In particular, agricultural waste attracts the attention of more and more researchers with its abundant natural resources, low cost, and good biocompatibility [18,19]. More importantly, using agricultural wastes as adsorbents is also beneficial for solving their own disposal problems, which greatly satisfies the conception of "treating wastes with wastes" [20]. Nowadays, more and more researchers have carried out relevant researches. However, as far as we know, these kinds of adsorbents are still in the stage of development. It is still a challenging task to develop new types of adsorbents with high adsorption capacity, good reusability, and environmental friendliness to remove Cd(II) from wastewater.

Sugarcane bagasse is a typical biomass waste widely produced from sugar and alcohol industries. There are approximately 5.2 million tons of sugarcane bagasse produced in China annually [21]. Despite some sugarcane bagasse was used for papermaking materials, fuel, or poultry feed, most sugarcane bagasse becomes waste in the market and factories, causing a huge waste of resources and a certain degree of environmental impact [22]. Therefore, it is urgent to develop effective and innovative ways to recycle sugarcane bagasse [23]. The composition of sugarcane bagasse is about 40%–50% cellulose, 25%–30% hemicelluloses, and 20%–25% lignin. The presence of these polymers causes the sugarcane bagasse rich in carboxyl, hydroxyl, and phenolic groups, which implies it can be exploited as an adsorbent for heavy metals removal [24,25]. There have been some studies on the adsorption of dyes and antibiotics by using sugarcane bagasse as an adsorbent [26]. However, there are few reports on the use of bagasse to remove heavy metals. The low efficiency of heavy metals removal may be due to the lack of good metal-binding sites on its surface [27]. In order to obtain an excellent adsorption effect, sugarcane bagasse can be chemically modified and loaded with functional groups of strong binding ability to heavy metals in biomass molecular structure to improve its adsorption performance for heavy metals [28].

Pyrzynsk pointed out that natural cellulose usually has very low ion exchange capacity, which can be enhanced by chemical modification and grafting, and the presence of carboxyl is the main part of heavy metal exchange sites [29]. Considering the aforementioned reasons, this study used sugarcane bagasse as raw material to prepare chemically modified adsorbent via carboxymethylation process, which introduced carboxyl group on the surface of natural sugarcane bagasse to increase the effective heavy metal adsorption site on the surface. Carboxymethylation is an effective method for preparing adsorbents with high-affinity carboxyl groups, which are used in various applications including the adsorption of heavy metal ions [30]. Maleic anhydride is a reactive monomer rich in carboxyl groups. However, up to date, there is no investigation on the potential of sugarcane bagasse modified with maleic anhydride in the adsorption of Cd(II).

In this study, we attempt to prepare environment-friendly carboxylate-functionalized sugarcane bagasse (CF-SCB) for achieving the reuse of bagasse and the remediation of heavy metal contamination simultaneously. After the carboxymethylation process, the sugarcane bagasse adsorbent was applied to adsorption Cd(II) from aqueous. To gain knowledge of the adsorption equilibrium behavior and binding mechanisms of Cd(II), the effect of several experimental parameters namely initial solution pH, adsorbent dosage, initial Cd(II) concentration, ionic strength, and contact time was investigated. Scanning electron microscopy (SEM), scanning electron microscopy with energy dispersive X-ray analysis (SEM-EDX), and Fourier transform infrared spectroscopy (FT-IR) were used to characterize the adsorbents. Regeneration and reuse of the adsorbent were also investigated to assess its potential use in several adsorption cycles.

2. Materials and methods

2.1. Materials

Sugarcane bagasse was collected from a sugar factory at LiuZhou, GuangXi, China. Maleic anhydride, cadmium(II) nitrate ($CdCl_2$, 99%), toluene, ethanol, hydrochloric acid (HCl, 37%), and sodium hydroxide (NaOH, 98%) were purchased from Guangzhou Chemical Reagent Factory (China). All the chemicals used were of analytical grade.

2.2. Preparation of SCB and CF-SCB

Sugarcane bagasse was washed with deionized water to remove impurities and dried in an oven at 70°C for 24 h until the evaporation of moisture. After that, the dried sugarcane bagasse was ground into a powder with a grinder and the particles of mesh size 0.15–0.25 mm were collected. Finally, the powder was again washed carefully with deionized water several times and then dried in an oven at 70°C to obtain the original sugarcane bagasse powder (SCB).

To prepare CF-SCB, sugarcane bagasse (10 g) was treated with 100 mL of aqueous NaOH solution (10 wt.%) at 25°C for 16 h under constant stirring. The suspension was filtered and washed up to neutral with distilled water. The washed material was then put in an oven at 90°C for 1 h to obtain mercerized bagasse. Afterward, the mercerized bagasse (6 g) and maleic anhydride (19.5 g) were immersed in toluene (100 mL) at 80°C. After 6 h, the product was filtered and washed in sequence with ethanol 80%, distilled water, saturated sodium bicarbonate, distilled water, and finally with acetone, and then dried to a constant weight at 70°C to obtain the pure CF-SCB.

2.3. Characterization of adsorbents

The structure and property of the adsorbent were evaluated by the Brunauer–Emmett–Teller (BET) analyzer. The surface morphology of the SCB and CF-SCB was analyzed by SEM (Merlin, Zeiss, DE) and elemental analysis was performed using an EDS spectrometer attached to SEM. The surface functional groups of CF-SCB before and

after adsorption were analyzed by using FT-IR spectroscopy (Nicolet 6700, Thermo Fisher Scientific, USA). The point of zero charges of each sample were determined via a Zeta potentiometer (Zetasizer Nano ZS, Malvern, UK).

2.4. Adsorption batch experiments

2.4.1. Effect of pH

25 mg CF-SCB was added in 100 mL Cd(II) solution with an initial concentration of 10 mg/L. The pH of the solution was in the range of 2.0–8.0 and this mixture was placed in an oscillating shaker at 150 rpm and 30°C for 8 h, the solution samples were collected for Cd(II) measurement.

2.4.2. Effect of adsorbent dosage

0.10–1.5 g/L of SCB and CF-SCB were mixed with 100 mL Cd(II) solution of 100 mg/L at pH 6.0. The mixture was shaken at 30°C with a speed of 150 rpm and solution samples were collected after 8 h.

2.4.3. Effect of ionic strength

Effects of K^+, Na^+, Mg^{2+}, and Ca^{2+} ranging from 0 to 0.2 mol/L on Cd adsorption were investigated. In the experiment, the dosage of CF-SCB was 0.2 g/L and the initial Cd concentration was 30 mg/L at pH 6.0. The adsorption reaction was conducted in the shaker for 8 h.

2.4.4. Adsorption isotherm experiment

25 mg CF-SCB was mixed with 50 mL Cd(II) solution at 5, 10, 25, 50, 100, 150, 200, 300, 400, and 600 mg/L which the solution pH was adjusted to 4.0 and 6.0. The reaction mixtures were shaken at 150 rpm for 16 h at 30°C.

2.4.5. Adsorption kinetics experiment

25 mg SCB and CF-SCB were mixed with a Cd(II) solution of 100 mL at 10 mg/L and pH 6.0. The reaction mixtures were then shaken at 150 rpm for 5, 15, 30, 45, 60, 90, 120, 150, 180, 240, 300, 360, 420, and 480 min at 20°C, 30°C, 40°C, and 50°C, respectively.

After adsorption, the solution was separated using 0.45 μm membrane filters (Millex, Millipore), the filtrate was analyzed immediately. The Cd(II) concentration was calculated by flame atomic absorption spectrophotometer. The removal rate (%) and adsorption capacity (q_e, mg/g) of Cd(II) onto SCB and CF-SCB were calculated by Eqs. (1) and (2):

$$\text{Removal rate} = \frac{C_0 - C_e}{C_0} \times 100\% \tag{1}$$

$$q_e = \frac{(C_0 - C_e) \times V}{m} \tag{2}$$

where C_0 and C_e (mg/g) are the Cd(II) concentrations in the initial and equilibrium states, respectively; V (L) is the solution volume and m (g) is the mass of the adsorbent.

In this series of adsorption batch experiments, the pH of each solution was adjusted by 0.1 M HCl and NaOH. Each experiment was repeated three times for reproducibility and accuracy.

2.5. Regeneration and reusability of CF-SCB

25 mg CF-SCB was added into 100 mL Cd(II) solution (10 mg/L) of pH 6.0. Then the mixture was shaken at 150 rpm at 30°C for 16 h, the removal rate of Cd(II) was calculated by using the Eq. (1). After adsorption, CF-SCB-Cd was collected, dried, and used for the further desorption experiment. The collected CF-SCB-Cd (25 mg) was then mixed with 0.1 mol/L hydrochloric acid solution (20 mL). The mixture was shaken at 150 rpm for 2 h at 30°C and then filtrated through a 0.45 μm membrane filter. The quantity of Cd(II) desorbed from CF-SCB-Cd could be calculated according to Eq. (3) [31]. The above process was repeated five times:

$$\text{Desorption efficiency} = \frac{\text{Amount of Cd desorbed}}{\text{Amount of Cd adsorbed}} \times 100\% \tag{3}$$

3. Results and discussion

3.1. Synthesis and characterization of CF-SCB

The synthesis process of CF-SCB is shown in Fig. 1. Firstly, the cellulose in the SCB was swelled by alkalization treatment to increase the separation of polysaccharide chains and destroy the internal hydrogen bond structure, which facilitated the maximum contact of the chemical reagents with the hydroxyl groups in the SCB composition during the chemical modification process. Then, the hydroxyl group in the molecular structure of the bagasse was esterified with maleic anhydride under high-temperature conditions by using low toxic toluene as a solvent. The hydroxyl groups at C-2, C-3, and C-6 of cellulose are reactive and can react with anhydride and the whole process can be regarded as the substitution of H in the hydroxyl group by the ester group in maleic anhydride [32]. Finally, after washing with saturated sodium bicarbonate, the carboxyl functionalized sugarcane bagasse (CF-SCB) was successfully prepared. It should be noted that the role of toluene as a solvent in the
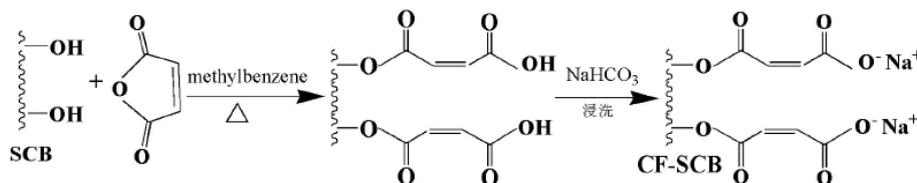
Fig. 1. Preparation procedure of CF-SCB.

carboxymethylation reaction is to provide accessibility of the maleic anhydride to the reaction centers of the cellulose chain rather than directly involved in the synthesis process [33].

The FTIR spectra for SCB, CF-SCB, and CF-SCB after Cd(II) adsorption (CF-SCB-Cd) are shown in Fig. 2. For raw SCB, The strong band at 3,430 cm^{-1} was due to the –OH symmetric stretching vibration of cellulose and lignin [34]. The distinct band at 2,980 and 1,170 cm^{-1} were attributed to the vibration of the C–H and C–O–C bond [35]. The characteristic bands of the five-member cyclic anhydride v_{C-O-C} has been observed at 1,400 cm^{-1} [36]. The appearance of the above characteristic peaks verified that the main components of bagasse were cellulose and hemicellulose. After chemical modification, there were shifts in the peak positions as their intensities were enhanced, and the presence of a characteristic band at 1,620 cm^{-1} was assigned to the asymmetric stretching modes of COO of the carboxylic acid salt and that at 1,480 cm^{-1} was due to CH$_2$ bending [37]. Besides, a broad adsorption band of C=C groups was seen at bands arising at 2,060 cm^{-1} [38], suggesting that the hydroxyl group in the molecular structure of bagasse has been esterified with maleic anhydride, and the ionized carboxyl group was successfully introduced into the molecular structure of bagasse.

The BET parameters, such as the pore structure parameters of SCB and CF-SCB are shown in Table 1. The total pore volume and surface area of SCB are 3.61 cm^3/g and 1.35 m^2/g, respectively. For the CF-SCB, the total pore volume and surface area reduce while the average pore diameter rises. During the alkalization treatment and chemical modification, it occurs the dissolution and elution of sucrose and soluble lignin in the SCB pore and increases

the average pore diameter [39]. Meanwhile, the esterification is favored to occurring the amorphous field of SCB and resulting in improving the regularity of CF-SCB. Therefore, the CF-SCB exhibits a more compact structure and obtains the different variations in BET data.

Morphological images of SCB and CF-SCB before and after sulfonation were analyzed by SEM; this is shown in Fig. 3. The SCB sample displays smooth and fine morphological appearances with regular shapes while the morphology of CF-SCB-Cd appears a significant shrunk with wrinkled surfaces. This phenomenon represented the process of attaching the –COOH functional group to the sugarcane bagasse. The wrinkled surfaces increased contacting area between Cd(II) and CF-SCB, helping to improve the adsorption of Cd(II) [40].

Furthermore, the true elemental compositions of all the samples are revealed by the EDS peaks. From the EDX graphs, it can be observed that the content of the O element increased from 45.56% to 49.20% for CF-SCB, while the content of the C element decreased from 54.44% to 46.98%. Meanwhile, it presents a new peak of the Na element in the SEM-EDS for CF-SCB. These results evidenced that –COONa was successfully introduced into the SCB molecular chain.

3.2. Optimization of the adsorption conditions

3.2.1. Effect of solution pH

pH usually plays a pivotal role in acquiring high Cd(II) adsorption capacity. It not only affects the form of pollutants in the adsorption process but also plays an important role in surface properties and ionization of adsorbents [41]. The zeta potential variation of CF-SCB and the effect of pH on the adsorption of Cd(II) by CF-SCB are shown in Fig. 4a. It can be noticed that the surface of CF-SCB adsorbent has a more negative charge, which should be ascribed to the presence of carboxyl groups on the surface of CF-SCB. The zeta potential of CF-SCB decreases with the pH increases from 2 to 8, indicating an increase in the degree of deprotonation of the carboxyl group.

When the pH ranges from 2 to 3, the removal rate of Cd(II) by CF-SCB slight increases from 7.56% to 8.13%. Interestingly, the Cd(II) adsorption ratio significantly increases to 91.87% when the pH value rises from 3 to 5. The results have shown that the adsorption behavior of CF-SCB adsorbent on Cd(II) is strongly dependent on the pH of the solution. With the increase of pH, the maximum adsorption capacity was obtained near a neutral environment (pH = 6, 7, and 8). Therefore, pH 6 was chosen as the initial pH value for the following experiments.

This adsorption phenomenon can be explained as follows: there are a large number of carboxyl groups on the CF-SCB surface, and the adsorption of Cd(II) is carried out by coordination between Cd ions and the carboxyl groups. At low solution pH (e.g., ≤3), the carboxyl groups on the CF-SCB surface were protonated by the large amount of H$^+$ in the solution, which hindered their binding with Cd(II) and resulting in the poor adsorption [42]. Furthermore, the surface of CF-SCB is surrounded by a large number of positive charges, the electrostatic repulsion is generated to the Cd(II) which results in the reduction of adsorption
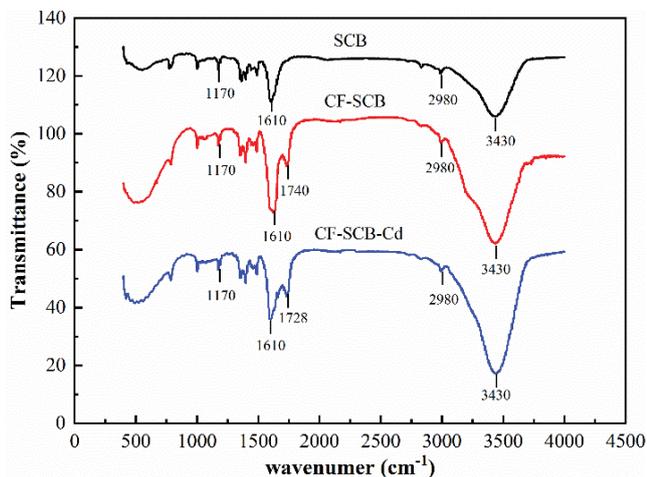
Fig. 2. FTIR spectra of SCB, CF-SCB, and CF-SCB-Cd.

Table 1
BET characteristics of SCB and CF-SCB

Sample	SCB	CF-SCB
Total pore volume (cm^3/g)	3.61	3.29
Surface area (m^2/g)	1.35	0.72
Average pore diameter (μm)	10.69	18.33
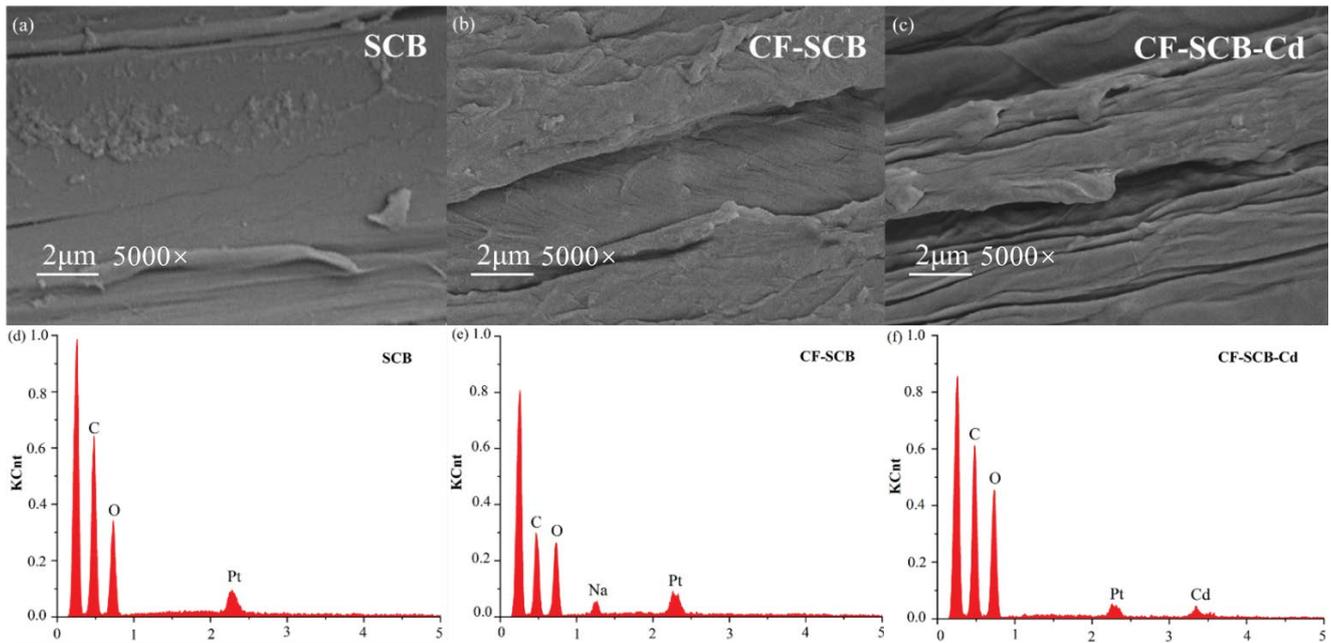
Fig. 3. SEM images and EDX elemental peaks of SCB and CF-SCB.
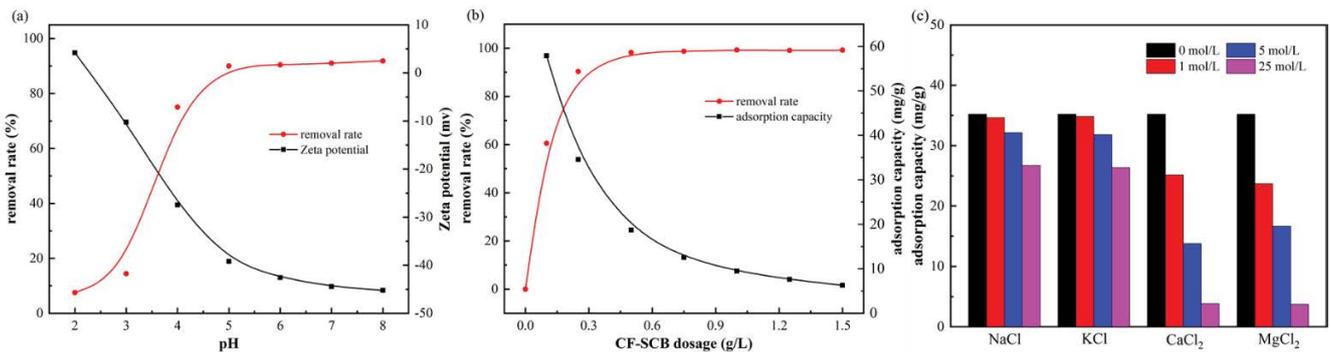
Fig. 4. Effect of pH (a), dosage (b), and ionic strength (c) on Cd(II) adsorption onto CF-SCB.

capacity. With the increase of the initial pH, the content of H^+ in the solution decreases gradually, and more carboxyl groups of CF-SCB exist in the form of COO^-, which will facilitate the combination of Cd(II) and ultimately increase the adsorption capacity [43].

3.2.2. Effect of adsorbent dosage

Since the effective surface area and binding sites affect the adsorption efficiency, it is important to choose the proper amount of initial adsorbent dosage [44]. From Fig. 4b, the percentage adsorption increases from 60.56% to 90.38% but adsorption density decreases from 60.56 to 36.15 mg/g when the adsorbent dose was increased from 0.1 to 0.25 g/L. This was because the increase of total surface area and active functional groups on CF-SCB provide more sites for Cd(II) adsorption [45]. However, upon increasing the CF-SCB dosage to 0.5–0.75 g/L, the removal efficiency did not get any further addition, the Cd(II) percentage removal and adsorption amount reached 90.38% and 36.15 mg/g respectively, and this might be due to the

saturation of active sites [46]. On the contrary of removal efficiency, the opposite trend could be observed on the adsorption capacity of Cd(II) by CF-SCB. Such changes could be explained by the per gram CF-SCB was surrounded by less and less Cd(II) as the amount of CF-SCB increases, making it more difficult for Cd to bind to the active sites on the surface of CF-SCB. In addition, the agglomeration of adsorbent would occur at high CF-SCB content in the solution, leading to a decrease in the number of effective sites on the surface of the adsorbent [47].

3.2.3. Effect of ionic strength

The heavy metal ions always co-exist with inorganic salts in wastewater in practice. Therefore, it is relatively necessary to find out the effect of ionic strength on Cd(II) removal is helpful for the restoration of polluted water. Fig. 4c illustrates the effect of ionic strength on Cd(II) adsorption. With ionic strength (NaCl, KCl, $CaCl_2$, and $MgCl_2$) increasing from 0 to 25 mmol/L, the Cd(II) adsorption removal decreased from 88.26% to 67.01%, 66.10%,

9.63%, and 9.23% indicating that the adsorption of Cd(II) was greatly affected by the ionic strength. The decrease of adsorption capacity may be due to the competition of Na^+, K^+, Ca^{2+}, and Mg^{2+} with Cd(II) for adsorption sites on CF-SCB. Furthermore, Ca^{2+} and Mg^{2+} with more positive charges would occupy more adsorption sites than Na^+ and K^+. Similar conclusions have been reported in many previous studies [48,49]. The negative effect of coexisting cation on Cd(II) adsorption was mainly due to the competitive adsorption, which confirmed that the adsorption of Cd(II) on CF-SCB was mostly through ion exchange mechanism more than surface complexation [50]. This result also consistent with the analysis of characterization above.

3.3. Process modeling

3.3.1. Adsorption isotherm studies

The adsorption isotherm reflects the distribution of the adsorbate molecules between the liquid phase and the solid phase when the adsorption process reaches equilibrium. It can reveal the type of adsorbate layer formed on the surface of the adsorbent, in addition, to being used to estimate the maximum adsorption of the adsorbent. Ability [51]. The adsorption isotherm data of Cd(II) on CF-SCB at pH = 4.0 and 6.0 is presented in Fig. 5a. And the control experiment using SCB was performed at pH = 6.0. As the Cd(II) concentration increases, the equilibrium adsorption capacity increased and reached saturation gradually. The maximum adsorption capacities of Cd(II) on CF-SCB were measured to be 124.48 and 108.80 mg/g at pH 6.0 and 4.0, respectively. While the maximum Cd(II) adsorption capacity onto SCB was only 13.60 mg/g which is only about one-tenth of that of CF-SCB adsorbent. Obviously, the presence of a carboxyl group can effectively increase the number of heavy metal-binding sites on the surface of CF-SCB and improve the Cd adsorption capacity.

For further study on the adsorption phenomenon, the collected isotherms experimental data have been fitted
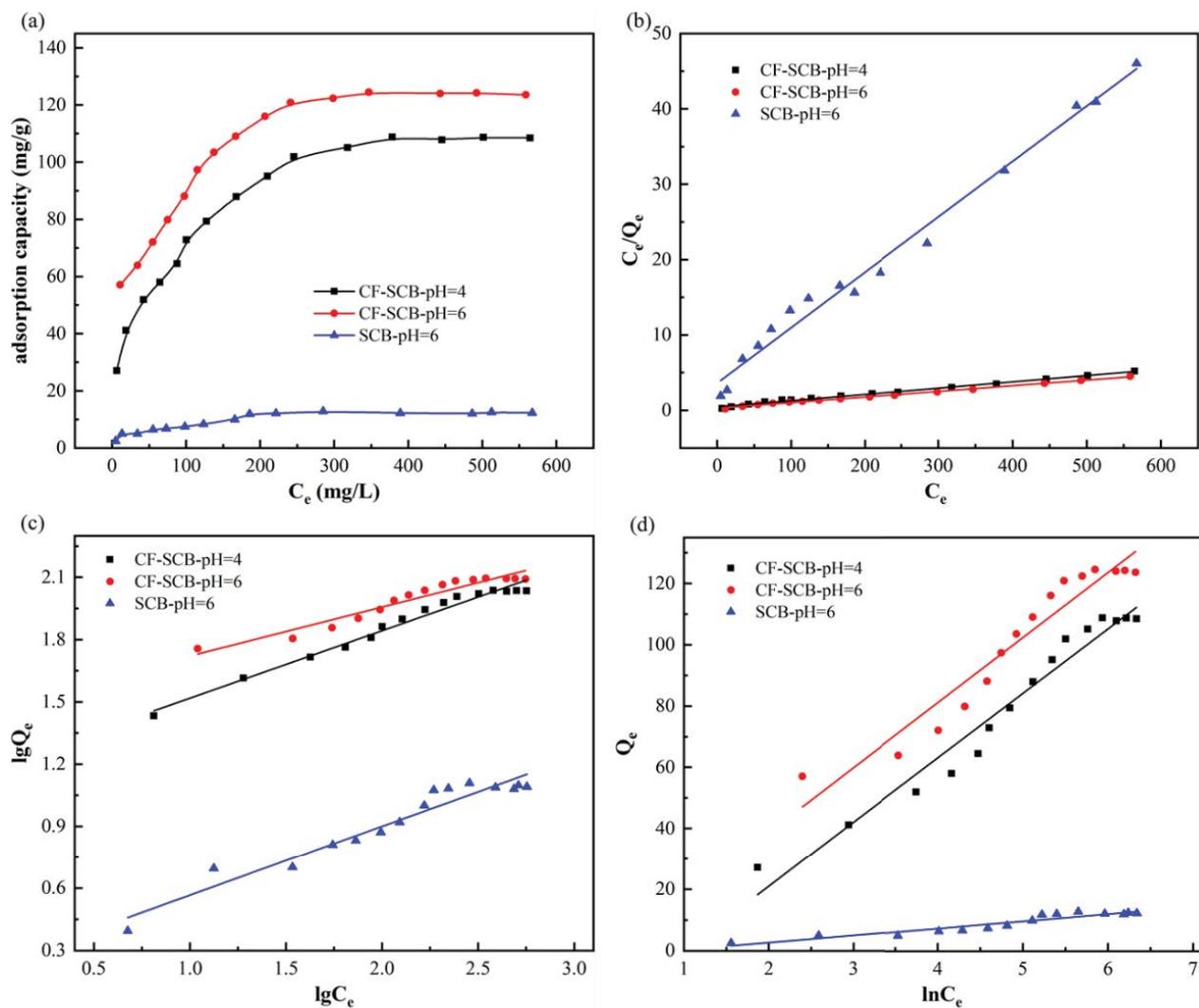
Fig. 5. (a) Adsorption isotherm of Cd(II) on CF-SCB and SCB, (b–d) fitting of the experimental adsorption isotherm data to the (b) Langmuir, (c) Freundlich, and (d) Temkin models.

with Langmuir, Freundlich, and Temkin models, respectively. The model equations are, respectively, expressed in Eqs. (4)–(6) [52]:

$$\frac{C_e}{q_e} = \frac{C_e}{q_m} + \frac{1}{K_L \cdot q_L} \tag{4}$$

$$\log q_e = \log K_F + \frac{1}{n}\log C_e \tag{5}$$

$$q_e = B\ln K_T + B\ln C_e \tag{6}$$

where q_e (mg/g) is the adsorption capacity at equilibrium; C_e (mg/L) is the concentration of the Cd(II) solution at equilibrium; q_m (mg/L) is the theoretical saturate adsorption capacity; and K_L (L/mg) is called affinity parameter for Langmuir models; K_F is the Freundlich isotherm constant and $1/n$ is the heterogeneity factor; K_T (mg/g) is Temkin isotherm constant and the constant B is related to the heat of adsorption.

The linear fitting of three adsorption isothermal model are shown in Figs. 5b–d, and the simulated parameters by the three models are all listed in Table 2. The Langmuir isotherm is obeyed better than the Freundlich and Temkin isotherms as is evident from the values of regression coefficients. The Langmuir model predicted the maximum equilibrium Cd(II) uptakes onto CF-SCB is 134.23 and

120.19 mg/g at pH 6 and 4 and it was very close to the experimentally obtained values. The results implied that the binding site (i.e., –COONa) on CF-SCB was uniformly distributed on the surface, and the absorption of Cd(II) on CF-SCB was considered to be monolayer adsorption [53].

In order to evaluate the adsorption performance of CF-SCB better, a comparison between CF-SCB and many previously reported Cd(II) adsorbents was also carried out, and the results are summarized in Table 3. This result suggesting CF-SCB is an efficient adsorbent for the removal of Cd(II) in wastewater, and compared to agricultural waste-based adsorbents previously reported, the adsorption capacity of CF-SCB is similar or higher than other reported adsorbents. Therefore, CF-SCB is an efficient adsorbent for the removal of Cd(II) in water due to its excellent adsorption performance, relatively simple, and low-cost modification process.

3.3.2. Adsorption kinetics studies

Adsorption kinetics can provide critical information on reaction rate and pathway, the residence time required to attain the equilibrium, and the possible mechanism, thus largely determine the potential application of the adsorbent [65]. The effect of contact time on Cd(II) adsorption by CF-SCB at four temperatures is shown in Fig. 6a. It can be observed that the adsorption rate of Cd(II) increased rapidly during the first 90 min, which was ~80% of the

Table 2
Isotherm parameters for the adsorption of Cd(II) onto CF-SCB and SCB

Samples	pH	Experimental	Langmuir			Freundlich			Temkin		
		q_{exp} (mg/g)	q_m (mg/g)	K_L (L/mg)	R^2	K_F (mg/g)	n	R^2	K_T (mg/L)	B	R^2
CF-SCB	4	108.80	120.19	0.019	0.994	15.604	3.079	0.977	0.374	21.028	0.959
	6	124.48	134.23	0.027	0.996	30.595	4.246	0.931	0.832	21.224	0.923
SCB	6	12.86	13.60	0.020	0.986	1.708	2.998	0.931	0.422	2.354	0.894

Table 3
Comparison of adsorption capacities among various waste-derived Cd(II) adsorbents

Adsorbent	q_{max} (mg/g)	pH	References
Modified corn stalk	12.73	7.0	[54]
Syzygium cumini L. leaf powder	29.08	5.5	[55]
Xanthated nano banana cellulose	156.26	6.0	[56]
Ginkgo biloba L. shells-based adsorbent	42.59	6.0	[57]
Burmese grape leaf extract	44.12	4.0	[58]
Acrylonitrile modified corncob-based biochars	85.65	6.8	[59]
Rice straw biochars prepared at 700°C	65.40	5.5	[60]
NaOH modified saw dust	73.62	5.0	[61]
NaOH treated rice husk	20.2	9.0	[62]
Nitric acid modified corncobs	19.3	8.0	[63]
Common reed activated with H_3PO_4	83.43	7.0	[64]
SCB	13.60	6.0	This work
CF-SCB	120.19/134.23	4.0/6.0	This work

equilibrium adsorption capacity of Cd(II). It is understood that the fast adsorption rate during the initial adsorption stage is attributed to a large number of effective adsorption sites [66]. As the adsorption process proceeds, the rate of increase became slower and the adsorption equilibrium reached after 180 minutes. Furthermore, the adsorption capacity of CF-SCB and the equilibrium adsorption amount enhanced with the increase of temperature. The equilibrium adsorption amounts were 34.72, 35.29, 36.16, and 37.38 mg/g at 20°C, 30°C, 40°C, and 50°C, respectively.

In order to investigate the adsorption kinetics of Cd(II) onto CF-SCB, pseudo-first-order, pseudo-second-order, and Elovich models were applied to analyze the experimental data. The model equations are respectively expressed in Eqs. (7)–(9) [67]:

$$\ln(q_e - q_t) = -k_1 t + \ln q_e \tag{7}$$

$$\frac{t}{q_t} = \frac{1}{q_e^2 \cdot k_2} + \frac{t}{q_e} \tag{8}$$

$$q_t = A + B \cdot \ln t \tag{9}$$

where q_e (mg/g) and q_t (mg/g) are the amounts of Cd(II) adsorbed on CF-SCB at equilibrium time and a certain time t (min), respectively; k_1 (min^{-1}) and k_2 (g/mg min) are the pseudo-first-order and pseudo-second-order equilibrium rate constants, respectively. A (mg/g) and B (mg/g min) are both the Elovich constants.

The predicted kinetics of Cd(II) adsorption on CF-SCB at four different temperatures were obtained and the result is shown in Figs. 6b–d. Simultaneously, all the parameters of the three adsorption kinetic models are shown in Table 4. Based on the analysis of correlation coefficient (R^2), it
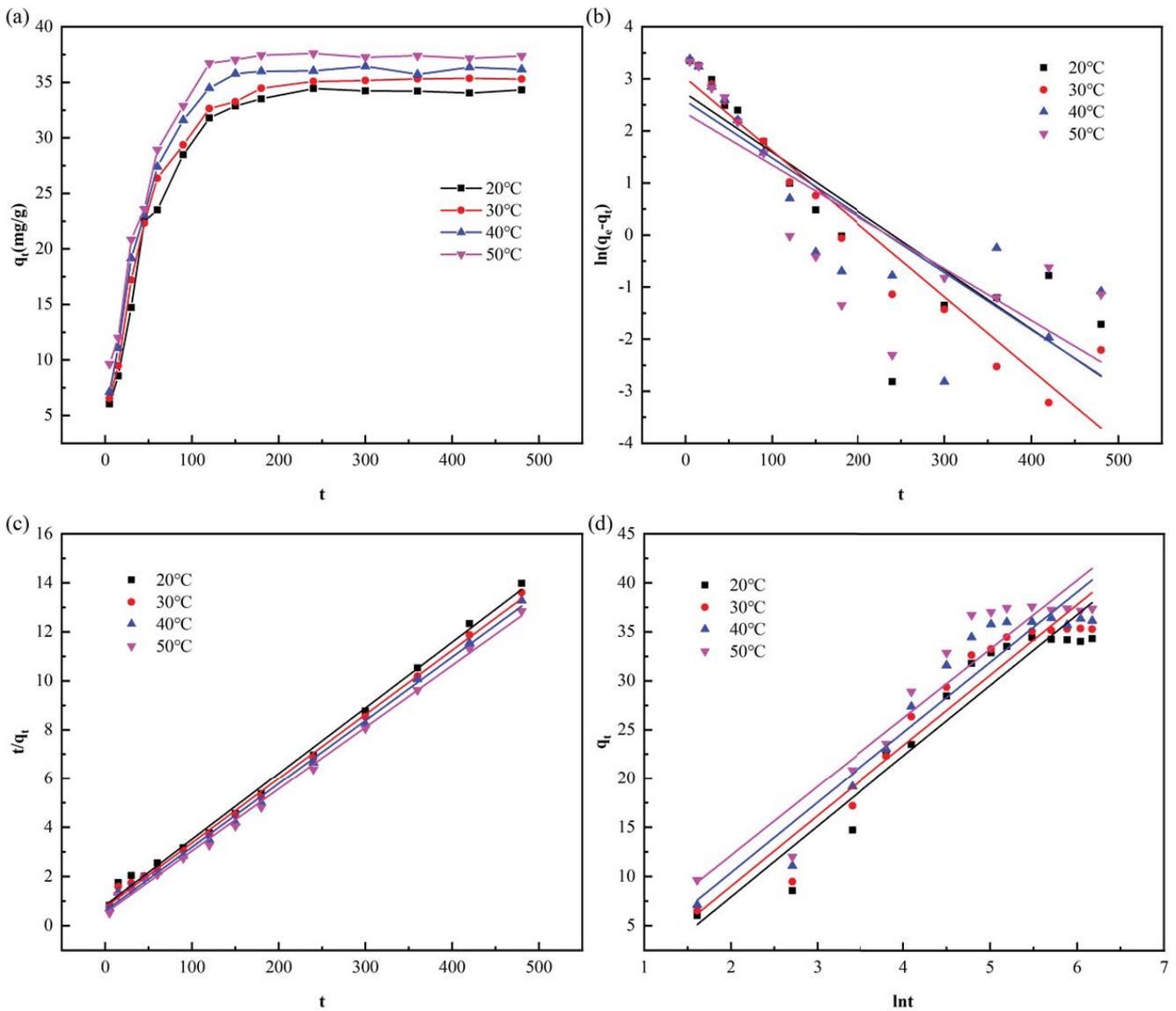
Fig. 6. (a) Adsorption kinetics of Cd(II) on CF-SCB, (b–d) linear fitting of the experimental adsorption isotherm data to the (b) pseudo-first-order, (c) pseudo-second-order, and (d) Elovich models.

was found that R^2 values for pseudo-second-order kinetic model are 0.996, 0.997, 0.997, and 0.998 at 20°C, 30°C, 40°C, and 50°C, respectively. That means adsorption kinetics of CF-SCB toward Cd(II) could well be approximated more favorably by pseudo-second-order model rather than pseudo-first-order model and Elovich model which supporting the presupposition that the adsorption is controlled by chemical adsorption involving valent forces [68].

3.3.3. Adsorption thermodynamics studies

Thermodynamic studies can be used to explore the feasibility of the adsorption process. The thermodynamic parameters of Cd(II) adsorption on CF-SCB were evaluated by experiments at different temperatures. The various thermodynamic parameters were calculated by Eqs. (10)–(12) [69]:

$$K_d = \frac{q_e}{C_e} \tag{10}$$

$$\ln K_d = \frac{\Delta S^\circ}{R} - \frac{\Delta H^\circ}{RT} \tag{11}$$

$$\Delta G^\circ = \Delta H^\circ - T\Delta S^\circ \tag{12}$$

where K_d is the distribution coefficient, R is the universal gas constant (8.314 J/mol K), T is the temperature (K). The van't Hoff plots of $\ln K_d$ against $1/T$ were produced which is shown in Fig.6a, and the values of ΔH° and ΔS° can be calculated according to the linear relationship between $\ln K_d$ and $1/T$.

The adsorption thermodynamic parameters at four temperatures are shown in Table 5. The ΔH° value was positive (20.08 kJ/mol), signifying the adsorption of Cd(II) by CF-SCB is an endothermic process. The positive ΔS° (83.28 J K/mol) confirmed the degree of disorder increase, which may correspond to structural changes in adsorbents or adsorbents [70]. In all cases, the ΔG° value was positive which indicating Cd(II) adsorption onto the CF-SCB was spontaneous. Simultaneously, the absolute value of ΔG° ascended with the increase of temperature, which further suggesting the adsorption process of Cd(II) becomes more feasible at high temperatures [71].

3.4. Regeneration and reusability evaluation of CF-SCB

Regeneration of adsorbent usually realizes the recovery of adsorption molecules, reuse of adsorbent, reduced

the cost of the adsorption process, and help to understand the mechanism of adsorption process well. Hence, a batch adsorption–desorption study was conducted to evaluate the reuse potential of CF-SCB in this study. The results of five adsorption–desorption cycles tests are given Fig. 7b. The adsorption efficiency of CF-SCB was decreased (only 10%) from 90.02% to 81.09% in the former two cycles and was remained at a good level at about 80% in the back of the three cycles. At the end of each cycle, the CF-SCB adsorbent exhibited a high percentage of desorption (over 96%). In other words, the regeneration and reuse efficiency of the adsorbent were reasonably good, even if adsorption uptake decreased slightly, desorption efficiency was fairly maintained after the fifth cycle. This result indicated that CF-SCB can be reused in wastewater treatment applications. The residual Cd on CF-SCB could be recovered by the vacuum distillation condensation method, and then incinerate as hazardous wastes to reduce damage to the environment [72–74].

3.5. Cost analysis

Generally speaking, the cost of adsorbent and its regeneration predominantly determine the cost of the adsorption process for Cd removal [52]. Based on the method described by Nordin et al. [75], Mashile et al. [76], and Argun et al. [77], Table S1 represented the cost estimation breakdown for the preparation of CF-SCB. Comparing to other commercial adsorbents, such as activated carbon (charcoal, activated coconut, EMD chemicals; $145/kg), an ion-exchange resin (Dowex(r) 50WX8-100; $390/kg) [77], the cost of CF-SCB is much cheaper. A kilogram of the prepared CF-SCB costs nearly CNY98.1 ($15.1, the economic indicators are converted from Chinese Yuan to Dollar at the exchange rate of 1$ = 6.5 CNY). It should be noted that the cost may be lower than CNY98.1/kg due to toluene as a solvent that could be reused after CF-SCB was filtered out from the solution. Moreover, the high adsorption capacity (134.23 mg/g) and good regeneration performance of

Table 5
Thermodynamic parameters for the adsorption of Cd(II) onto CF-SCB at different temperatures

Temperature (K)	ΔG° (kJ/mol)	ΔH° (kJ/mol)	ΔS° (kJ/mol)
293	−4.43	20.08	83.28
303	−5.04		
313	−6.06		
323	−7.04		

Table 4
Kinetic parameters for the adsorption of Cd(II) onto CF-SCB at different temperatures

Temperature (°C)	Experimental	Pseudo-first-order		Pseudo-second-order			Elovich		
	q_{exp} (mg/g)	k_1 (min^{-1})	R^2	q_e (mg/g)	$k_2 \times 10^{-3}$ (g/mg min)	R^2	A (mg/g)	B (mg/g min)	R^2
20	34.72	0.86	0.754	37.47	0.85	0.996	0.06	7.25	0.921
30	35.29	0.97	0.937	38.05	0.94	0.997	0.07	7.19	0.928
40	36.16	0.85	0.729	38.51	1.17	0.997	0.08	7.15	0.899
50	37.38	0.79	0.636	39.51	1.26	0.997	0.11	7.03	0.895

CF-SCB further reduced the cost of CF-SCB, since one batch can be reused at least five times with a slight adsorption capacity loss (<11.6%). Therefore, CF-SCB is an economical material with a simple synthesis process and excellent adsorption capacity.

3.6. Adsorption mechanism

The characteristic peaks of the carboxyl group near 1,620 and 1,480 cm^{-1} shifted to 1,610 and 1,490 cm^{-1} respectively after the adsorption process, indicating that there exists a coordination interaction between the carboxyl and Cd^{2+} ions [78]. From the EDX diagram in Fig.1, after adsorption, the Na peak in the CF-SCB sample disappeared while the Cd peak emerged, and the amount of cd increase is almost the same as the amount of Na reduction. That means Na(I) was fully displaced in exchange by Cd(II) during the adsorption.

Based on all the above studies, a surface ion-exchange mechanism was proposed to describe the adsorption of Cd on CF-SCB (Fig. 8). When the CF-SCB was added to the Cd solution, –COONa ionized in solution. Upon displacement of Na(I) ions, the carboxyl groups on the adsorbent become negatively charged and thus ready to attract the positively charged Cd(II) ions. It indicated that each metal species was trapped between the two carboxyl binding sites on the adsorbent due to appropriate spatial arrangement. Hence, ion exchange was considered to be the main binding mechanism for Cd(II) adsorption in this study, and similar results were obtained in other studies involving carboxyl groups [79,80].

4. Conclusions

In summary, a new type of agricultural waste-based adsorbent (CF-SCB) has been synthesized to remove Cd(II)
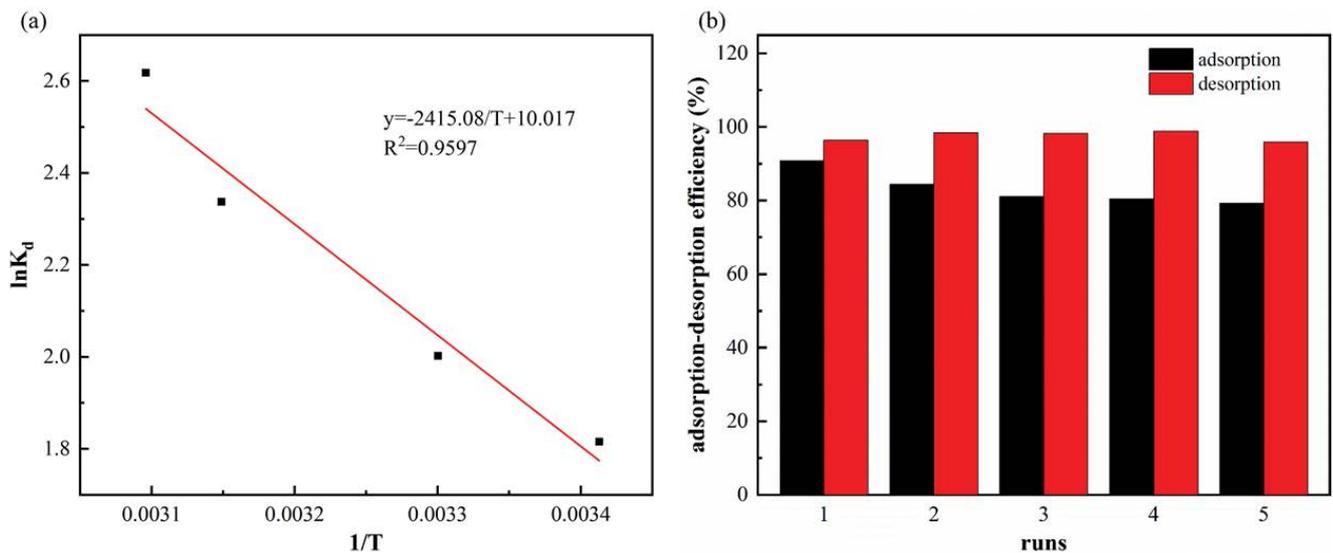
Fig. 7. (a) Thermodynamic plots for Cd(II) adsorption on CF-SCB and (b) adsorption and desorption efficiency of CF-SCB.
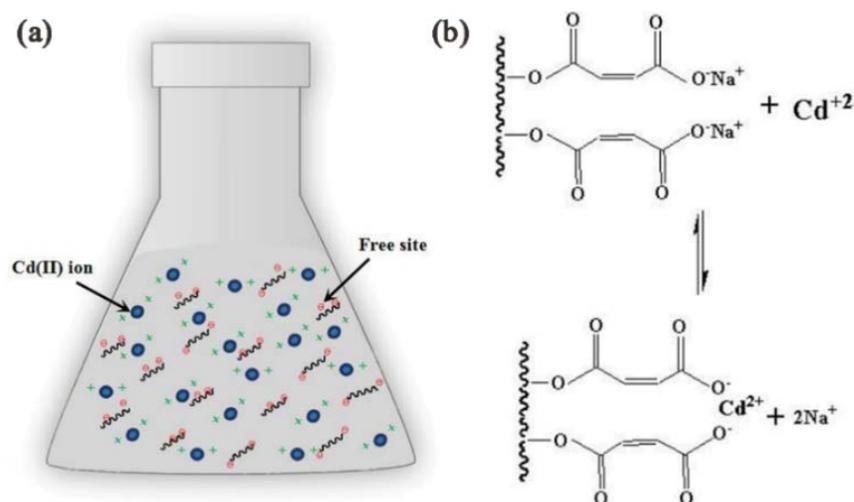
Fig. 8. Adsorption mechanisms of Cd(II) onto CF-SCB: (a) electrostatic attraction and (b) ion exchange.

from an aqueous solution in order to realize the purpose of "treating waste with waste." Batch adsorption experiments showed that the CF-SCB exhibited excellent performance for Cd(II) removal from aqueous solution with high adsorption capacity (134.23 mg/g at pH 6).

Adsorption isotherm and kinetic studies showed that the experimental data agree well with the Langmuir isotherm model and the pseudo-second-order kinetic model. Simultaneously, the thermodynamic parameters indicated that the adsorption process was a spontaneous, endothermic, and entropy increasing process. Furthermore, the CF-SCB has a good regeneration and reuse efficiency after five cycles. A combined analysis of batch experiments and characterizations of CF-SCB substantiated that ion exchange between Na^+ and Cd^{2+} played a key role in the absorption process of Cd(II).

Based on all facts, CF-SCB was proved to be an effective and alternative adsorbent for the removal of Cd(II) from acidic and weak acidic polluted water/wastewater in low salt concentration due to its good adsorption qualities as well as low-cost.

Acknowledgments

References

[1] F.L. Fu, Q. Wang, Removal of heavy metal ions from wastewaters: a review, J. Environ. Manage., 92 (2011) 407–418.
[2] D.A. Glatstein, F.M. Francisca, Influence of pH and ionic strength on Cd, Cu and Pb removal from water by adsorption in Na-bentonite, Appl. Clay Sci., 118 (2015) 61–67.
[3] S. Hokkanen, A. Bhatnagar, M. Sillanpaa, A review on modification methods to cellulose-based adsorbents to improve adsorption capacity, Water Res., 91 (2016) 156–173.
[4] J. Liang, X.M. Li, Z.G. Yu, G.M. Zeng, Y. Luo, L.B. Jiang, Z.X. Yang, Y.Y. Qian, H.P. Wu, Amorphous MnO_2 modified biochar derived from aerobically composted swine manure for adsorption of Pb(II) and Cd(II), ACS Sustainable Chem. Eng., 5 (2017) 5049–5058.
[5] M.F. Zhu, L. Zhu, J.L. Wang, T.L. Yue, R.H. Li, Z.H. Li, Adsorption of Cd(II) and Pb(II) by *in situ* oxidized Fe_3O_4 membrane grafted on 316L porous stainless steel filter tube and its potential application for drinking water treatment, J. Environ. Manage., 196 (2017) 127–136.
[6] M.J. Amiri, R. Roohi, A. Gil, Numerical simulation of Cd(II) removal by ostrich bone ash supported nanoscale zero-valent iron in a fixed-bed column system: utilization of unsteady advection-dispersion-adsorption equation, J. Water Process Eng., 25 (2018) 1–14.
[7] Z.B. Shang, L.W. Zhang, X.Y. Zhao, S.H. Liu, D.L. Li, Removal of Pb(II), Cd(II) and Hg(II) from aqueous solution by mercapto-modified coal gangue, J. Environ. Manage., 231 (2019) 391–396.
[8] Y.D. Zou, X.X. Wang, A. Khan, P.Y. Wang, Y.H. Liu, A. Alsaedi, T. Hayat, X.K. Wang, Environmental remediation and application of nanoscale zero-valent iron and its composites for the removal of heavy metal ions: a review, Environ. Sci. Technol., 50 (2016) 7290–7304.
[9] A. Habineza, J. Zhai, T. Ntakirutimana, F.P. Qiu, X.T. Li, Q.F. Wang, Heavy metal removal from wastewaters by agricultural waste low-cost adsorbents: hindrances of adsorption technology to the large scale industrial application-a review, Desal. Water Treat., 78 (2017) 192–214.
[10] Y.H. Li, F.Q. Liu, B. Xia, Q.J. Du, P. Zhang, D.C. Wang, Z.H. Wang, Y.Z. Xia, Removal of copper from aqueous solution by carbon nanotube/calcium alginate composites, J. Hazard. Mater., 177 (2010) 876–880.
[11] M.W. Yap, N.M. Mubarak, J.N. Sahu, E.C. Abdullah, Microwave induced synthesis of magnetic biochar from agricultural biomass for removal of lead and cadmium from wastewater, J. Ind. Eng. Chem., 45 (2017) 287–295.
[12] A.K. Thakur, G.M. Nisola, L.A. Limjuco, K.J. Parohinog, R.E.C. Torrejos, V.K. Shahi, W.J. Chung, Polyethylenimine-modified mesoporous silica adsorbent for simultaneous removal of Cd(II) and Ni(II) from aqueous solution, J. Ind. Eng. Chem., 49 (2017) 133–144.
[13] M.C. Tonucci, L.V.A. Gurgel, S.F. de Aquino, Activated carbons from agricultural byproducts (pine tree and coconut shell), coal, and carbon nanotubes as adsorbents for removal of sulfamethoxazole from spiked aqueous solutions: kinetic and thermodynamic studies, Ind. Crop Prod., 74 (2015) 111–121.
[14] L.B.L. Lim, N. Priyantha, D.T.B. Tennakoon, M.K. Dahri, Biosorption of cadmium(II) and copper(II) ions from aqueous solution by core of *Artocarpus odoratissimus*, Environ. Sci. Pollut. Res., 19 (2012) 3250–3256.
[15] W.J. Yin, C.C. Zhao, J.T. Xu, J. Zhang, Z.Z. Guo, Y.H. Shao, Removal of Cd(II) and Ni(II) from aqueous solutions using activated carbon developed from powder-hydrolyzed-feathers and Trapa natans husks, Colloid Surf., A, 560 (2019) 426–433.
[16] A. Baruah, S. Mondal, L. Sahoo, U.K. Gautam, Ni–Fe-layered double hydroxide/N-doped graphene oxide nanocomposite for the highly efficient removal of Pb(II) and Cd(II) ions from water, J. Solid State Chem., 280 (2019) 164–170.
[17] Z.H. Yang, X.H. Chen, S.Y. Li, W.H. Ma, Y. Li, Z.D. He, H.R. Hu, T. Wang, Effective removal of Cd(II) from aqueous solution based on multifunctional nanoporous silicon derived from solar kerf loss waste, J. Hazard. Mater., 385 (2020), doi: 10.1016/j.jhazmat.2019.121522.
[18] T.A.H. Nguyen, H.H. Ngo, W.S. Guo, J. Zhang, S. Liang, Q.Y. Yue, Q. Li, T.V. Nguyen, Applicability of agricultural waste and by-products for adsorptive removal of heavy metals from wastewater, Bioresour. Technol., 148 (2013) 574–585.
[19] W.J. Liu, L.L. Ling, Y.Y. Wang, H. He, Y.R. He, H.Q. Yu, H. Jiang, One-pot high yield synthesis of Ag nanoparticle-embedded biochar hybrid materials from waste biomass for catalytic Cr(VI) reduction, Environ. Sci. Nano, 3 (2016) 745–753.
[20] T.T. Luo, X.K. Tian, C. Yang, W.J. Luo, Y.L. Nie, Y.X. Wang, Polyethylenimine-functionalized corn bract, an agricultural waste material, for efficient removal and recovery of Cr(VI) from aqueous solution, J. Agric. Food Chem., 65 (2017) 7153–7158.
[21] C.R. Nie, X. Yang, N.K. Niazi, X.Y. Xu, Y.H. Wen, J. Rinklebe, Y.S. Ok, S. Xu, H.L. Wang, Impact of sugarcane bagasse-derived biochar on heavy metal availability and microbial activity: a field study, Chemosphere, 200 (2018) 274–282.
[22] A.K. Varma, P. Mondal, Pyrolysis of sugarcane bagasse in semi batch reactor: effects of process parameters on product yields and characterization of products, Ind. Crop Prod., 95 (2017) 704–717.
[23] Y. Li, L.Y. Hu, B.L. Shen, C.L. Dai, Q.J. Xu, D.Y. Liu, J. Jiang, Y. Li, M.W. Xu, Rib-like hierarchical porous carbon as reservoir for long-life and high-rate Li-Te batteries, Electrochim. Acta, 250 (2017) 10–15.
[24] H.C. Tao, H.R. Zhang, J.B. Li, W.Y. Ding, Biomass based activated carbon obtained from sludge and sugarcane bagasse for removing lead ion from wastewater, Bioresour. Technol., 192 (2015) 611–617.
[25] C.A. Rezende, M.A. de Lima, P. Maziero, E.R. de Azevedo, W. Garcia, I. Polikarpov, Chemical and morphological characterization of sugarcane bagasse submitted to a delignification process for enhanced enzymatic digestibility, Biotechnol. Biofuels, 4 (2011) 1–18.
[26] N. Rattanachueskul, A. Saning, S. Kaowphong, N. Chumha, L. Chuenchom, Magnetic carbon composites with a hierarchical structure for adsorption of tetracycline, prepared from sugarcane bagasse via hydrothermal carbonization coupled

with simple heat treatment process, Bioresour. Technol., 226 (2017) 164–172.

[27] Y. Liu, Q. Gao, S. Pu, H.Q. Wang, K.S. Xia, B. Han, C.G. Zhou, Carboxyl-functionalized lotus seedpod: a highly efficient and reusable agricultural waste-based adsorbent for removal of toxic Pb^{2+} ions from aqueous solution, Colloid Surf., A, 568 (2019) 391–401.

[28] M.J. Alves, I.V. Cavalcanti, M.M. de Resende, V.L. Cardoso, M.H. Reis, Biodiesel dry purification with sugarcane bagasse, Ind. Crop Prod., 89 (2016) 119–127.

[29] K. Pyrzynska, M. Trojanowicz, Functionalized cellulose sorbents for preconcentration of trace metals in environmental analysis, Crit. Rev. Anal. Chem., 29 (1999) 313–321.

[30] C.Q. Wang, H. Wang, Carboxyl functionalized *Cinnamomum camphora* for removal of heavy metals from synthetic wastewater-contribution to sustainability in agroforestry, J. Cleaner Prod., 184 (2018) 921–928.

[31] M.V. Subbaiah, D.S. Kim, Adsorption of methyl orange from aqueous solution by aminated pumpkin seed powder: kinetics, isotherms, and thermodynamic studies, Ecotoxicol. Environ. Saf., 128 (2016) 109–117.

[32] A. Hashem, S.M. Badawy, S. Farag, L.A. Mohamed, A.J. Fletcher, G.M. Taha, Non-linear adsorption characteristics of modified pine wood sawdust optimised for adsorption of Cd(II) from aqueous systems, J. Environ. Chem. Eng., 8 (2020), doi: 10.1016/j.jece.2020.103966.

[33] V. Pushpamalar, S.J. Langford, M. Ahmad, Y.Y. Lim, Optimization of reaction conditions for preparing carboxymethyl cellulose from sago waste, Carbohydr. Polym., 64 (2006) 312–318.

[34] J.B. Pang, F.L. Fu, Z.C. Ding, J.W. Lu, N. Li, B. Tang, Adsorption behaviors of methylene blue from aqueous solution on mesoporous birnessite, J. Taiwan Inst. Chem. Eng., 77 (2017) 168–176.

[35] X. Xie, H. Gao, X. Luo, T. Su, Y. Zhang, Z. Qin, Polyethyleneimine modified activated carbon for adsorption of Cd(II) in aqueous solution, J. Environ. Chem. Eng., 7 (2019), doi: 10.1016/j.jece.2019.103183.

[36] E.A. Ali, S.S. Elkholy, R.E. Morsi, M.Z. Elsabee, Studies on adsorption behavior of Cu(II) and Cd(II) onto aminothiophene derivatives of Styrene Maleic anhydride copolymer, J. Taiwan Inst. Chem. Eng., 64 (2016) 325–335.

[37] S. Yang, M.X. Hua, L. Shen, X.L. Han, M.Y. Xu, L.J. Kuang, D.B. Hua, Phosphonate and carboxylic acid co-functionalized MoS_2 sheets for efficient sorption of uranium and europium: multiple groups for broad-spectrum adsorption, J. Hazard. Mater., 354 (2018) 191–197.

[38] J.K. Bediako, W. Wei, S. Kim, Y.S. Yun, Removal of heavy metals from aqueous phases using chemically modified waste Lyocell fiber, J. Hazard. Mater., 299 (2015) 550–561.

[39] J.H. Wen, Y. Yin, X.F. Peng, S.D. Zhang, Using H_2O_2 to selectively oxidize recyclable cellulose yarn with high carboxyl content, Cellulose, 26 (2019) 2699–2713.

[40] J.K. Bediako, W. Wei, Y.S. Yun, Low-cost renewable adsorbent developed from waste textile fabric and its application to heavy metal adsorption, J. Taiwan Inst. Chem. Eng., 63 (2016) 250–258.

[41] M. Arshadi, F. Mousavinia, M.J. Amiri, A.R. Faraji, Adsorption of methyl orange and salicylic acid on a nano-transition metal composite: kinetics, thermodynamic and electrochemical studies, J. Colloid Interface Sci., 483 (2016) 118–131.

[42] M.F. Zou, X.Y. Chen, X.J. Lin, M.Y. Chen, N.N. Ding, L.Y. Yang, X.K. Ouyang, Fabrication of magnetic carboxyl-functionalized attapulgite/calcium alginate beads for lead ion removal from aqueous solutions, Int. J. Biol. Macromol., 120 (2018) 789–800.

[43] X.J. Li, C.J. Yan, W.J. Luo, Q. Gao, Q. Zhou, C. Liu, S. Zhou, Exceptional cerium(III) adsorption performance of poly(acrylic acid) brushes-decorated attapulgite with abundant and highly accessible binding sites, Chem. Eng. J., 284 (2016) 333–342.

[44] S. Wong, H.H. Tumari, N. Ngadi, N.B. Mohamed, O. Hassan, R. Mat, N.A.S. Amin, Adsorption of anionic dyes on spent tea leaves modified with polyethyleneimine (PEI-STL), J. Cleaner Prod., 206 (2019) 394–406.

[45] Y.Y. Su, Y.B. Jiao, C.C. Dou, R.P. Han, Biosorption of methyl orange from aqueous solutions using cationic surfactant-modified wheat straw in batch mode, Desal. Water Treat., 52 (2014) 6145–6155.

[46] R. Lavanya, T. Gomathi, K. Vijayalakshmi, M. Saranya, P.N. Sudha, S. Anil, Adsorptive removal of copper(II) and lead(II) using chitosan-g-maleic anhydride-g-methacrylic acid copolymer, Int. J. Biol. Macromol., 104 (2017) 1495–1508.

[47] C.F. Tang, Y. Shu, R.Q. Zhang, X. Li, J.F. Song, B. Li, Y.T. Zhang, D.L. Ou, Comparison of the removal and adsorption mechanisms of cadmium and lead from aqueous solution by activated carbons prepared from *Typha angustifolia* and *Salix matsudana*, Rsc Adv., 7 (2017) 16092–16103.

[48] Y. Xu, Y.G. Liu, S.B. Liu, X.F. Tan, G.M. Zeng, W. Zeng, Y. Ding, W.C. Cao, B.H. Zheng, Enhanced adsorption of methylene blue by citric acid modification of biochar derived from water hyacinth (*Eichornia crassipes*), Environ. Sci. Pollut. Res., 23 (2016) 23606–23618.

[49] L. Wang, J. Zhang, R. Zhao, C. Li, Y. Li, C.L. Zhang, Adsorption of basic dyes on activated carbon prepared from *Polygonum orientale* Linn: equilibrium, kinetic and thermodynamic studies, Desalination, 254 (2010) 68–74.

[50] B. Li, J. Guo, K. Lv, J. Fan, Adsorption of methylene blue and Cd(II) onto maleylated modified hydrochar from water, Environ. Pollut., 254 (2019), doi: 10.1016/j.envpol.2019.113014.

[51] Y.B. Wang, Y. Xie, Y.K. Zhang, S.Y. Tang, C.C. Guo, J.S. Wu, R. Lau, Anionic and cationic dyes adsorption on porous poly-melamine-formaldehyde polymer, Chem. Eng. Res. Des., 114 (2016) 258–267.

[52] X.J. Li, Z.M. Wang, J.L. Ning, M.M. Gao, W.B. Jiang, Z.D. Zhou, G.Y. Li, Preparation and characterization of a novel polyethyleneimine cation-modified persimmon tannin bioadsorbent for anionic dye adsorption, J. Environ. Manage., 217 (2018) 305–314.

[53] Q. Gao, J.F. Xie, Y.T. Shao, C. Chen, B. Han, K.S. Xia, C.G. Zhou, Ultrafast and high-capacity adsorption of Gd(III) onto inorganic phosphorous acid modified mesoporous SBA-15, Chem. Eng. J., 313 (2017) 197–206.

[54] L.C. Zheng, Z. Dang, X.Y. Yi, H. Zhang, Equilibrium and kinetic studies of adsorption of Cd(II) from aqueous solution using modified corn stalk, J. Hazard. Mater., 176 (2010) 650–656.

[55] K.S. Rao, S. Anand, P. Venkateswarlu, Modeling the kinetics of Cd(II) adsorption on *Syzygium cumini* L leaf powder in a fixed bed mini column, J. Ind. Eng. Chem., 17 (2011) 174–181.

[56] S.S. Pillai, B. Deepa, E. Abraham, N. Girija, P. Geetha, L. Jacob, M. Koshy, Biosorption of Cd(II) from aqueous solution using xanthated nano banana cellulose: equilibrium and kinetic studies, Ecotoxicol. Environ. Saf., 98 (2013) 352–360.

[57] Z.H. Wang, D.K. Shen, F. Shen, C.F. Wu, S. Gu, *Ginkgo biloba* L. shells-based adsorbent for the removal of Cu^{2+} and Cd^{2+} from aqueous solution: kinetics, isotherm, thermodynamics and mechanisms, J. Mol. Liq., 241 (2017) 603–611.

[58] R. Borah, D. Kumari, A. Gogoi, S. Biswas, R. Goswami, J.H. Shim, N.A. Begum, M. Kumar, Efficacy and field applicability of Burmese grape leaf extract (BGLE) for cadmium removal: an implication of metal removal from natural water, Ecotoxicol. Environ. Saf., 147 (2018) 585–593.

[59] M.K. Luo, H. Lin, B. Li, Y.B. Dong, Y.H. He, L. Wang, A novel modification of lignin on corncob-based biochar to enhance removal of cadmium from water, Bioresour. Technol., 259 (2018) 312–318.

[60] Y.Y. Deng, S. Huang, D.A. Laird, X.G. Wang, Z.W. Meng, Adsorption behaviour and mechanisms of cadmium and nickel on rice straw biochars in single- and binary-metal systems, Chemosphere, 218 (2019) 308–318.

[61] S.Q. Memon, N. Memon, S.W. Shah, M.Y. Khuhawar, M.I. Bhanger, Sawdust—A green and economical sorbent for the removal of cadmium(II) ions, J. Hazard. Mater., 139 (2007) 116–121.

[62] U. Kumar, M. Bandyopadhyay, Sorption of cadmium from aqueous solution using pretreated rice husk, Bioresour. Technol., 97 (2006) 104–109.

[63] R. Leyva-Ramos, L.A. Bernal-Jacome, I. Acosta-Rodriguez, Adsorption of cadmium(II) from aqueous solution on natural and oxidized corncob, Sep. Purif. Technol., 45 (2005) 41–49.

[64] M.Y. Abdelnaeim, I.Y. El Sherif, A.A. Attia, N.A. Fathy, M.F. El-Shahat, Impact of chemical activation on the adsorption performance of common reed towards Cu(II) and Cd(II), Int. J. Miner. Process., 157 (2016) 80–88.

[65] F. Mashkoor, A. Nasar, Preparation, characterization and adsorption studies of the chemically modified *Luffa aegyptica* peel as a potential adsorbent for the removal of malachite green from aqueous solution, J. Mol. Liq., 274 (2019) 315–327.

[66] X.C. Jin, Z.Y. Xiang, Q.G. Liu, Y. Chen, F.C. Lu, Polyethyleneimine-bacterial cellulose bioadsorbent for effective removal of copper and lead ions from aqueous solution, Bioresour. Technol., 244 (2017) 844–849.

[67] Q. Gao, H. Zhu, W.J. Luo, S. Wang, C.G. Zhou, Preparation, characterization, and adsorption evaluation of chitosan-functionalized mesoporous composites, Microporous Mesoporous Mater., 193 (2014) 15–26.

[68] Y.S. Ho, G. McKay, The kinetics of sorption of divalent metal ions onto sphagnum moss peat, Water Res., 34 (2000) 735–742.

[69] A. Roy, B. Adhikari, S.B. Majumder, Equilibrium, kinetic, and thermodynamic studies of azo dye adsorption from aqueous solution by chemically modified lignocellulosic jute fiber, Ind. Eng. Chem. Res., 52 (2013) 6502–6512.

[70] J.X. Yang, G.B. Hong, Adsorption behavior of modified *Glossogyne tenuifolia* leaves as a potential biosorbent for the removal of dyes, J. Mol. Liq., 252 (2018) 289–295.

[71] Y. Tian, X.F. Wang, Y.F. Pan, Simple synthesis of Ni-containing ordered mesoporous carbons and their adsorption/desorption of methylene orange, J. Hazard. Mater., 213 (2012) 361–368.

[72] D.C.R. Espinosa, J.A.S. Tenório, Fundamental aspects of recycling of nickel–cadmium batteries through vacuum distillation, J. Power Sources, 135 (2004) 320–326.

[73] D.C.R. Espinosa, J.A.S. Tenório, Recycling of nickel–cadmium batteries using coal as reducing agent, J. Power Sources, 157 (2006) 600–604.

[74] M. Assefi, S. Maroufi, Y. Yamauchi, V. Sahajwalla, Pyrometallurgical recycling of Li-ion, Ni–Cd and Ni–MH batteries: a minireview, Curr. Opin. Green Sustainable Chem., 24 (2020) 26–31.

[75] A.H. Nordin, S. Wong, N. Ngadi, M. Mohammad Zainol, N.A.F. Abd Latif, W. Nabgan, Surface functionalization of cellulose with polyethyleneimine and magnetic nanoparticles for efficient removal of anionic dye in wastewater, J. Environ. Chem. Eng., 9 (2021), doi: 10.1016/j.jece.2020.104639.

[76] G.P. Mashile, K.M. Dimpe, P.N. Nomngongo, A biodegradable magnetic nanocomposite as a superabsorbent for the simultaneous removal of selected fluoroquinolones from environmental water matrices: isotherm, kinetics, thermo-dynamic studies and cost analysis, Polymers, 12 (2020), doi: 10.3390/polym12051102.

[77] M.E. Argun, S. Dursun, M. Karatas, Removal of Cd(II), Pb(II), Cu(II) and Ni(II) from water using modified pine bark, Desalination, 249 (2009) 519–527.

[78] T.A. Saleh, V.K. Gupta, Processing methods, characteristics and adsorption behavior of tire derived carbons: a review, Adv. Colloid Interface Sci., 211 (2014) 93–101.

[79] Z.L. Du, T. Zheng, P. Wang, L.L. Hao, Y.X. Wang, Fast microwave-assisted preparation of a low-cost and recyclable carboxyl modified lignocellulose-biomass jute fiber for enhanced heavy metal removal from water, Bioresour. Technol., 201 (2016) 41–49.

[80] V.V. Kulkarni, A.K. Golder, P.K. Ghosh, Synthesis and characterization of carboxylic cation exchange bio-resin for heavy metal remediation, J. Hazard. Mater., 341 (2018) 207–217.

Supporting information

S1. Cost analysis

The unit cost analysis for modification of 1 kg adsorbent (CNY/kg) was calculated using the following equation:

$$\text{Unit cost}\left(\frac{\text{CNY}}{\text{kg}}\right) = \frac{\left(C_m \times V_m\right)}{M_a} \tag{S1}$$

where C_m is the cost of modificant solution as CNY/L or CNY/kg, V_m represent modificant volume or mass as L or kg, and M_a is the mass of used adsorbent as kg.

Table S1
Cost estimation breakdown for the production of CF-SCB

Process	Material	Measurement unit	Amount	Unit cost (CNY)	Price (CNY)
Preparation of CF-SCB	Sugarcane bagasse	kg	1	0	0
	Maleic anhydride	kg	3.25	5.2	16.9
	Toluene	L	16.7	4.2	70.14
	NaOH	kg	1	2.1	2.1
Net amount of 1 kg CF-SCB	–	–	–	–	89.1
Overhead cost (10% of net cost)	–	–	–	–	8.91
Total cost	–	–	–	–	98.1